Available online at www.CivileJournal.org

Civil Engineering Journal

(E-ISSN: 2476-3055; ISSN: 2676-6957)

Vol. 10, No. 08, August, 2024

Flexural Performance of Beams Strengthened with FRP Laminates and Alternative U-Wrap Anchors

Sneha M. Varghese [1*], Kiran Kamath [2], Rajiv Selvam [3], Surumi Rasia Salim [4]

[1] *Department of Civil Engineering, Manipal Academy of Higher Education, Dubai Academic City, Dubai, 345050, UAE.*

[2] *Department of Civil Engineering, Manipal Institute of Technology, Manipal Academy of Higher Education, Manipal 576104, India.*

[3] *Department of Mechanical Engineering, Manipal Academy of Higher Education, Dubai Academic City, Dubai, 345050, UAE.*

[4] *Department of Civil Engineering, University of Calgary, Calgary, T2N 1N4, Canada.*

Received 18 May 2024; Revised 20 July 2024; Accepted 25 July 2024; Published 01 August 2024

Abstract

Premature debonding is identified as the main failure mode in reinforced concrete (RC) beams strengthened with externally bonded Fiber-Reinforced Polymer (FRP) laminates. This issue leads to the underutilization of FRP materials and needs to be addressed. Research has shown that end anchorage systems can effectively delay/mitigate delamination failures and enhance the performance of strengthened beams. FRP U-wraps are an effective means to prevent debonding failure; however, as open-form anchors, U-wraps cannot always guarantee complete resistance to debonding failures. This study proposes an alternative U-wrapping technique where the ends of the U-wraps are flared and inserted into the concrete substrate. The feasibility and effectiveness of this technique were studied by comparing it with conventional U-wraps. The experimental phase involved testing seven RC beams, each measuring 1.96×0.15×0.3 meters, under four-point bending. The results showed that the anchorage technique improved beam performance in terms of load-deflection behavior, failure modes, ductility, and FRP strain. Additionally, finite element simulations were conducted using Abaqus software to assess the effectiveness of the alternative U-wrap scheme. These models incorporated various nonlinear material constitutive laws, including cohesive zone modeling to replicate debonding failures at the CFRP-concrete interface. The numerical predictions were found to be in good agreement with the experimental test data.

Keywords: Fiber Reinforced Polymer (FRP); Premature Debonding; Alternative U-Jackets; Finite Element Study; Abaqus.

1. Introduction

Fiber Reinforced Polymers (FRP) have emerged as highly effective retrofitting solutions, enhancing flexural strength, shear and axial capacity, torsional performance, seismic resilience, and overall durability of structural components [1, 2]. The process of externally bonding FRP composites with adhesives is widely used and is called the Externally Bonded Reinforcement (EBR) technique [3]. The flexural capacity of members can be increased by attaching FRP strips to the beam soffits using high-strength epoxy resins. Even though the method has promising advancements, it is accompanied by premature brittle debonding failure. The bonded FRP soffit plates debond with maximum strains far below the maximum tensile rupture strain, thereby impeding the effective use of FRP material. Hence, strengthening limits are imposed in EB-FRP structures by design codes [4]. Various endeavors are proposed to address the debonding failures and to facilitate effective stress transfer at critical locations. One of the most effective approaches to mitigate or avert catastrophic debonding failure and improve the efficiency of EBR strengthening is to use an end anchoring system. Many end anchorage systems are proposed to date to improve FRP-concrete bond strength. Some of them include FRP U-jackets [5], mechanical fasteners [6], and FRP spike and patch anchors [7, 8].

* Corresponding author: sneha.marium@dxb.manipal.edu

http://dx.doi.org/10.28991/CEJ-2024-010-08-01

FRP U-jackets are widely recognized as effective end anchorage systems for enhancing the performance of externally bonded reinforcement (EBR) specimens. Debonding typically manifests in two forms: concrete cover separation (CCS) and intermediate crack (IC) debonding. Applying FRP U-wraps at the ends of beams can prevent CCS failure, while placing them at regular intervals along the span can mitigate IC debonding failure. U-wraps offer essential confinement, reducing crack propagation and tensile peeling stresses at the ends or along the length of the beams. They improve load capacity, strain compatibility, ductility, and debonding strength of the elements. A study by Abdalla et al. [9] observed that beams with vertical U-wraps exhibited a 36% increase in yielding and a 35% increase in peak load compared to unanchored specimens, with higher deflection. The U-wraps effectively resisted debonding failure propagation from the plate ends and supported additional loads, enhancing the strain compatibility between the FRP and the substrate.

Various parametric studies are carried out to improve the existing U-wraps. Factors like width/area, material, and configuration are the main parameters considered. Chen et al. [10] studied the structural performance of beams reinforced with Basalt FRP (BFRP) soffit plates and U-jackets. An enhancement in FRP strain was observed, and the failure mode shifted from premature debonding to a less critical FRP rupture. This illustrates the superiority of BFRP over other FRP materials (like glass, carbon, and aramid). Other factors, like width/area of the FRP anchor, can eliminate plate end debonding and, as a result, lead the specimens to gradually experience IC debonding [11]. Fu et al. [12] concluded that an appropriately wide vertical U-jacket can minimize the possibility of CCS failure by reducing the interfacial stress between the longitudinal FRP and the concrete substrate. Finite element analysis performed on vertical U-jackets with Abaqus software revealed that their performance is influenced by the dimensions of the anchors, specifically their height, width, and thickness. It is important to note that using the minimum required area is optimal, as increasing the area does not significantly enhance load capacity [13].

Fu et al. [14] highlighted that the 45° inclined U-jacket improves the load-carrying capacity and ductility of RC beams when compared to the 90° and 135° U-jackets. The inclined U-wraps were capable of transferring the tensile strength of longitudinal FRP to the beam sides, lessening the interfacial stresses between substrate and FRP soffit plate. Because of the constraint offered by the inclined U-wraps, the beams were able to support additional load even after the IC debonding of the soffit plate until the eventual debonding of the U-jacket [15]. Flexural tests conducted by Al-Saawani et al. [16] on CFRP-strengthened beams using 45-degree inclined U-wraps with an area increase ranging from 33% to 100% demonstrated enhanced performance. The anchors effectively prevented CCS failure and supported loads exceeding the theoretically predicted IC debonding load, thereby delaying IC debonding failure.

The introduction of end anchorages has significantly enhanced the load capacity of strengthened beams; however, they have not substantially improved the ductility and deformability of the specimens [17–19]. FRP debonding contributes to reduced ductility in structural elements. The open design of FRP U-jackets makes them particularly vulnerable to debonding, which may limit their effectiveness in enhancing structural performance. To address this issue, researchers have developed various novel end anchorage techniques to maximize the benefits of existing systems [20, 21]. This study aims to contribute to the continual efforts towards creating reliable and efficient end anchorage techniques for strengthening and retrofitting RC structures with FRP materials. An alternative U-wrap mechanism is introduced with the aim of improving ductility, load transfer, bond strength, and reducing the risk of debonding. This study evaluates the viability and effectiveness of these modified alternative U-wraps through an experimental program, examining their impact on load capacity, failure modes, strain distribution, and ductility. The performance of the modified U-wraps is compared to that of standardized U-wrap anchors. Additionally, simulation studies using Abaqus software are conducted to validate the experimental results. Figure 1 illustrates the flowchart depicting the process of the methodology.

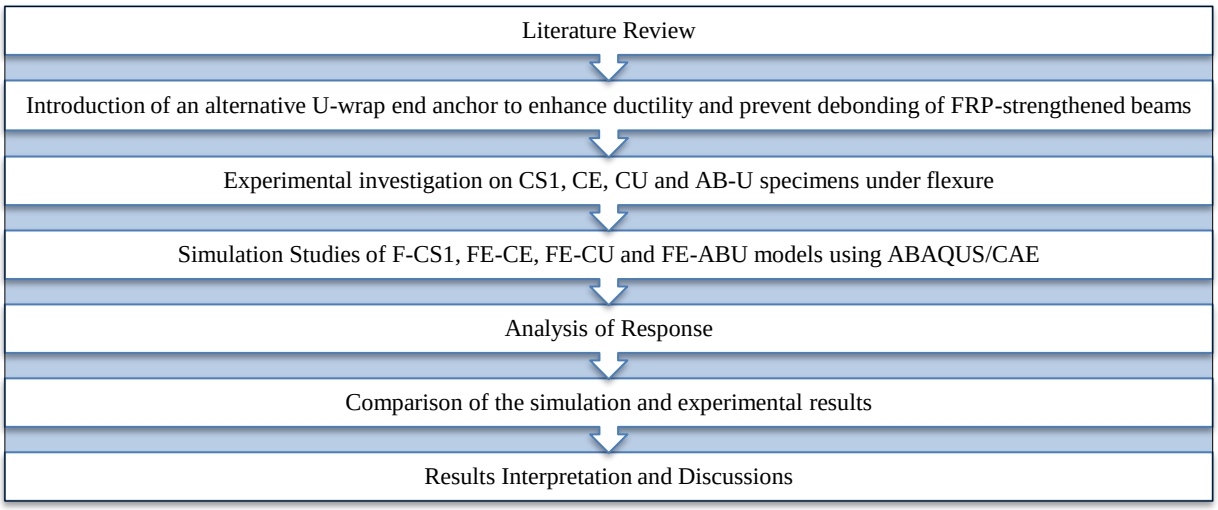

Figure 1. Flowchart depicting the workflow

2. Experimental Program

2.1. Test Matrix

This research investigated the flexural behavior of reinforced concrete beams (RC beams) with and without end anchorages. Seven full-size beams were prepared for experimental analysis under four-point bending. Based on the strengthening techniques used, the beams were divided into four groups. These include a control sample—an unstrengthened beam, designated as CS-1. All other test specimens were strengthened with CFRP laminates externally bonded to the soffit of the beam, with two groups featuring end anchors. The test specimens CE1 and CE2 are reinforced only with CFRP soffit plates. In contrast, the test specimens CU1 and CU2 are reinforced with CFRP soffit plates and U-shaped end anchorages. The specimens designated as AB-U1 and AB-U2 are strengthened with externally bonded CFRP soffit plates and alternative U-jacket end anchorage systems. The test matrix of the experimental study is shown in Table 1.

Table 1. Test Matrix of Experimental Study

S: No.	Specimen ID	Number of specimens	Details-Strengthening Technique
1	CS	1	Control Specimen-Unstrengthened
2	CE	2	EBR Specimen-Beams equipped with CFRP soffit plate only
3	CU	2	Beams equipped with CFRP soffit plate and conventional U-jacket anchors
4	AB-U	2	Beams equipped with CFRP soffit plate and alternative U-jacket anchors

2.2. Design of Specimens

The behavior of beam specimens under flexure is investigated in this study using four-point bending loading. All beams have similar geometry, with a total length of 1960 mm and a cross-section of 0.15×0.3 m. The clear span of the specimens is 1860 mm. A total of 4 deformed rebars were used as longitudinal reinforcement, which includes two numbers of 12 mm diameter tension rebars and two numbers of 10 mm diameter compression rebars. Shear reinforcement consisted of two-legged 10 mm diameter stirrups, positioned at 150 mm center-to-center spacing. The thickness of the concrete cover was 50 mm along the length and 25 mm at the cross-section. Except for the control specimen (CS-1), CFRP laminates were installed on the underside of all test specimens. The CFRP laminates have a length of 1460 mm and a width of 100 mm. Test specimens CU1 and CU2 are wrapped with 100 mm-wide conventional vertical U-shaped end anchors made of CFRP. The alternative 100 mm wide U-wrap anchors used for AB-U1 and AB-U2 are created by cutting the edges of the U-wrap strips into flares and inserting the flared ends into 30 mm diameter holes on the sides of the concrete beam specimens. The specimen details are shown in Figure 2, and the beam layouts are shown in Figure 3.

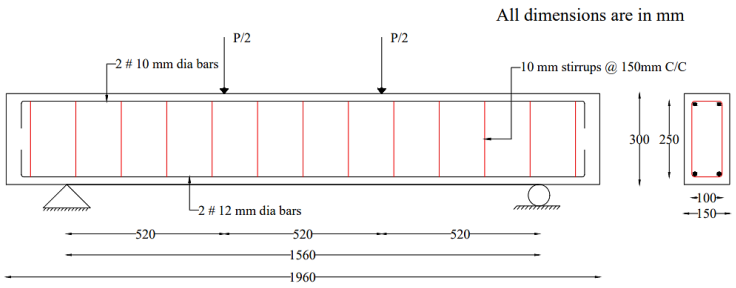

Figure 2. Geometry of Specimens and Reinforcement Details (mm)

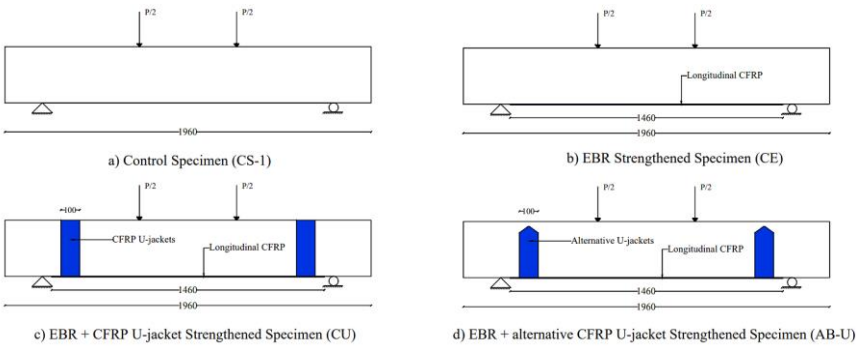

Figure 3. Layouts of Specimens (dimensions in mm): a) Control Specimen (CS1); b) EBR strengthened beam (CE); c) EBR + CFRP U-jackets strengthened beam (CU); d) EBR + alternative CFRP U-jacket strengthened beam (AB-U)

2.3. Material Properties

All specimens were cast using the same batch of concrete and similar curing conditions to ensure uniform concrete characteristics. The concrete mix was created with a water-cement ratio of 0.35. Cylinders, cubes, and prisms as per standard specifications were cast to determine the modulus of elasticity, compressive strength, and splitting tensile strength of the concrete, respectively. The average compressive strength of six cubes, each measuring 0.15×0.15×0.15m and cured under the same conditions, was found to be 50.6 MPa. The elastic modulus of the concrete is 36.3 GPa, and its tensile strength is 4.33 MPa. Uniaxial Tensile testing was performed to determine the characteristics of both 10 mm and 12 mm deformable bars used as internal reinforcements. The average yield strength and tensile strength of 10 mm bars are reported as 528 MPa and 616 MPa, respectively. The equivalent values for 12 mm bars are 560 MPa and 645 MPa, respectively. The elasticity modulus and Poisson's ratio for both types of bars are 200 GPa and 0.3, respectively.

For external reinforcement, commercially available unidirectional CFRP fabrics, SikaWrap®-300 C, were employed. According to the manufacturer's specifications, the laminate's nominal design thickness, average tensile strength, and average elastic modulus are 0.167 mm, 3.5 GPa, and 220 GPa, respectively. The maximum break elongation is 1.59%. The CFRP fabric is securely bonded to the concrete substrate using Sikadur®-330, a two-part epoxy adhesive composed of resin and hardener. The adhesive has a modulus of elasticity of 4.5 GPa, a tensile strength of 30 MPa, and a 0.9% tensile strain at break.

2.4. Preparation of Specimens and Strengthening

The reinforced beam specimens were cast and properly cured for 28 days. Necessary surface preparations were carried out on the beam specimens before bonding the CFRP fabrics. Mechanical grinders were used to remove laitance, imperfections, or flaws on the substrate and to achieve an open-textured surface. The exterior sharp edges were rounded to avoid stress concentration. Wire brushes and vacuum cleaners were employed to ensure a dust-free surface for smooth epoxy application. Holes were drilled in the AB-U1 and AB-U2 specimens to accommodate the ends of the alternative U-wraps. Air blowers were used to remove dust and other particles from the holes. The wet layup method was used to bond the CFRP fabrics. Sikadur®-330, a two-part epoxy adhesive, was used as both primer and impregnating resin. The epoxy was mixed according to the manufacturer's specifications and applied as a primer coat on the soffit and at the allocated U-wrap application points on the beam specimens. The CFRP fabrics were cut, impregnated with resin, and then applied to the substrate. Excess resin and air bubbles were wiped off the surface using rollers. The strengthened specimens were cured at room temperature before testing.

The operations carried out for the specimen fabrication is shown in Figures 4 and 5 represents the surface preparation and process of wet layup application of CFRP specimens.

Figure 4. Casting of concrete beams

Figure 5. Externally Bonding CFRP to concrete Substrate

2.5. Alternative U-wrap Strengthening

Conventional U-wrap anchors cannot completely prevent debonding. Moreover, enhancing the interfacial bond behavior between the FRP and concrete is essential for preventing debonding failures. In this study, an alternative method to the U-wrap technique was presented, which can delay debonding at the panel ends and mitigate the associated disadvantages. After installing the laminates on the soffit of the beams, the position of the U-wraps was determined. Modifications were made to the U-jackets to create the alternative U-wrapping end anchorage scheme. To implement this end anchorage scheme, the following steps were carried out:

- To create the end anchorage, CFRP fabric strips of required dimensions (10 cm wide and 75 cm long) were cut.
- The ends of each strip were cut into 5 cm long protrusions/flares on both sides, as shown in Fig. 3(a). The flared CFRP strips were impregnated with epoxy resin, and the flared ends of the strips were inserted into the beam sides.
- To insert the flared ends of the alternative U-jackets, 3 cm holes were drilled on both sides of the specimen's web. The centerline of the holes was 50 mm below the top edge of the beams.
- The flared ends were inserted into the cleaned and vacuumed holes and secured with additional epoxy resin.

The details of the installation of an alternative U-wrap are depicted in Fig. 3. Special care must be taken during the cutting process of CFRP fabrics. The non-homogeneous and anisotropic behavior of FRP fabrics can result in material wear and fiber pullouts. To ensure minimal distortion of fibers, high-quality and sharp cutting equipment (fabric scissors) was used in the study. The details of the installation of an alternative U-wrap are depicted in Figure 6. Figure 7 depicts finished, strengthened specimens used in the study.

Figure 6. Steps of Alternative U-wrap Installation a) CFRP fabric cut at ends b) Installation of CFRP soffit laminate c) Installation of end anchors d) The flared ends of the anchor inserted to the precut holes at beam sides

Figure 7. Finished Specimen: AB-U Specimen (view from beam bottom)

2.6. Test Setup and Instrumentation

The flexural load tests were conducted on all specimens using a 4-point bending setup. Each beam had a total span of 1960 mm and was supported by roller and pinned supports at the ends, providing an effective span of 1560 mm. Figure 5(a) illustrates the schematic diagram of the test setup. The distance between the loading points was set at one-third of the effective span, which is 520 mm. The testing apparatus included a SCHIMADZU Universal Testing Machine with a 1000 kN capacity, connected to a data acquisition system for capturing load displacement curves and strain values. To measure displacements, three linear variable displacement transducers (LVDTs) were placed at the center of the span and at the load application points. After mounting the specimens to the testing frame, electrical strain gauges with a resistance of 120 Ω and a gauge length of 30 mm were attached to monitor strain development on the CFRP soffit plate. Three strain gauges were bonded to the soffit plate at the ends and the center.

All displacement sensors and strain gauges were connected to the data acquisition system to monitor strain and displacement readings simultaneously. A longitudinal spreader beam was employed to ensure uniform load distribution to the loading points. A load cell of 200 kN was placed above the spreader beam and is used to obtain data externally from the data acquisition system. The specimens were subjected to displacement-controlled loading at a rate of 1.5 mm/min. Figure 8 shows the schematic representation of the flexural loading test setup, and the instrumentation details are shown in Figure 9.

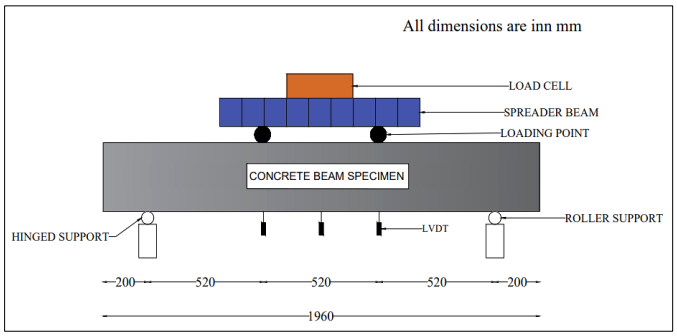

Figure 8. Schematic representation of Loading frame setup b) Experimental setup and details of instrumentation

Figure 9. Test setup with beam specimen for flexural loading

3. Experimental Results and Discussions

The main results of this experimental investigation include load bearing capacity, maximum strain, displacement ductility, and the mode of failure of the beam specimens. The efficacy of the adopted alternative U-wrap scheme can be thoroughly examined by comparing it with the control specimens.

3.1. Load Deflection Behavior

The load versus midspan deflection for each specimen group is presented in Figures 10 and 11. The load-deflection (L-D) curves display a trilinear pattern. In the initial phase, the L-D curve demonstrates linear behavior, reflecting the elastic performance of the specimens prior to cracking. In the second phase, the curve remains linear but with reduced

steepness and stiffness, indicating cracking in the tension zone. This is followed by a stage where steel yielding occurs. The CFRP-strengthened specimens exhibit a significant decline in strength and displacement due to the debonding of the longitudinal CFRP from the concrete substrate. Key results from the L-D curves are presented below.

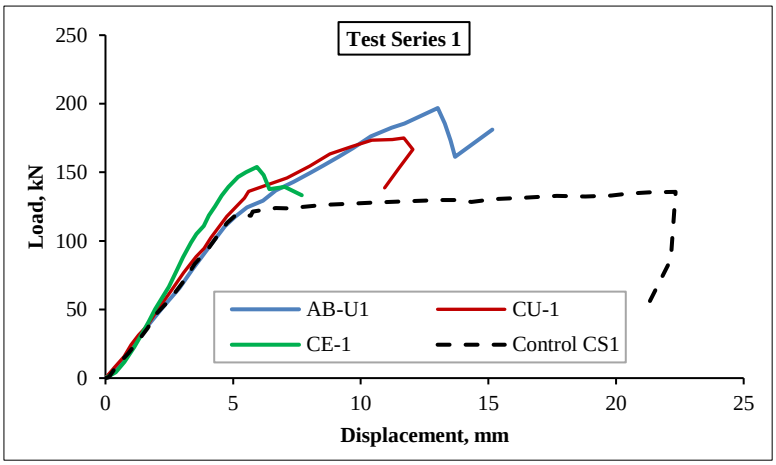

Figure 10. Load v/s midspan deflection curves of experimental study: Test series 1

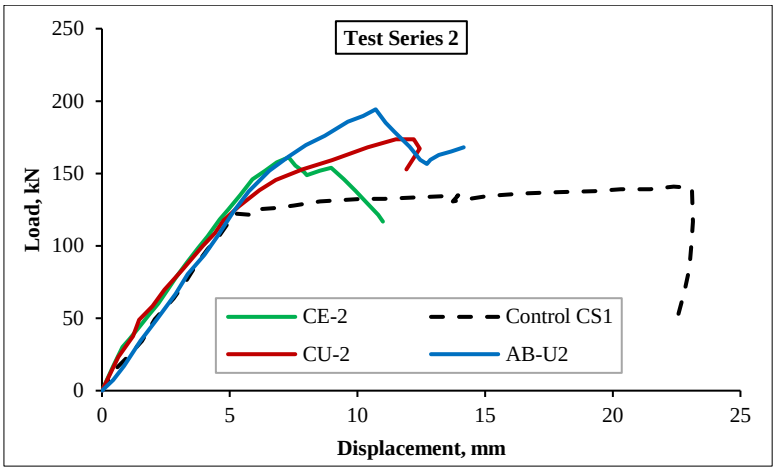

Figure 11. Load v/s midspan deflection curves of experimental study: Test series 2

The unstrengthened RC beam specimen CS-1 achieved an ultimate load capacity of 135.1 kN and a maximum displacement of 21.25 mm. Specimens CE1 and CE2, which were strengthened with only longitudinal CFRP fabrics, reached ultimate loads of 155.9 kN and 149 kN, respectively, with corresponding displacements of 6.73 mm and 6.9 mm. The addition of CFRP in the tension zone resulted in a 13.5% increase in flexural capacity, demonstrating the effectiveness of CFRP strengthening. Specimens CU1 and CU2, which included U-wrap end anchorages, further improved ultimate loads to 173.51 kN and 175 kN, respectively, showing a 14.3% increase over the CE specimens. This suggests that FRP U-jackets are more effective at sustaining residual loads even after the failure of longitudinal CFRP. The alternative U-wrap scheme used in specimens AB-U1 and AB-U2 led to even greater load capacities of 194.45 kN and 198.1 kN, with maximum displacements of 13.1 mm and 12.6 mm. The alternative U-wraps shifted the debonding failure and improved flexural capacity by 13% compared to conventional U-wrap end anchors. Additionally, the load-deflection curves of the strengthened beams are stiffer than those of the unstrengthened specimen CS-1. The highest stiffness was noticed in the AB-U specimens, as the anchors provide adequate bonding, which restricts flexural cracks.

3.2. Failure Modes

From the visual observations, it is observed that the reference beam CS-1 experienced typical flexural failure, as illustrated in Figure 12-a. The failure initiated with vertical cracks on the beam's tension side, which further propagated across the moment zone. This failure mode resulted from the yielding of tensile reinforcement followed by concrete crushing. Sudden debonding failures were observed in specimens CE1 and CE2, even though they achieved higher peak loads when compared to CS-1 specimens. Concrete cover separation failure is noted in these specimens, as shown in Figure 13-a. Longitudinal CFRP and the concrete cover debond from the plate ends when a major crack propagates to the mid-span. These discontinuities cause peak shear stresses to develop at the CFRP sheet ends, which are then

transferred to the concrete substrate. As a result, the concrete cover separates along with the CFRP, leading to cover separation failure. Specimens with U-jacket end anchors (CU) successfully mitigated cover separation failure, shifting the failure mode to intermediate crack (IC) debonding, as depicted in Figure 14-a. The CU1 and CU2 specimens experienced IC debonding followed by complete detachment of the longitudinal CFRP; however, the U-jackets continued to carry additional load until complete beam failure.

(a)

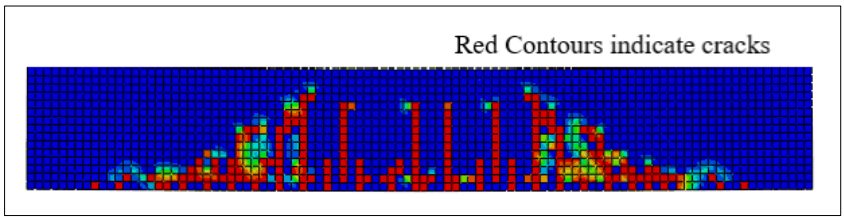

(b)

Figure 12. (a) Failure mode in control specimen CS - Flexural Failure, (b) Failure mode in control specimen FE-CS - Flexural Failure (Numerical Study)

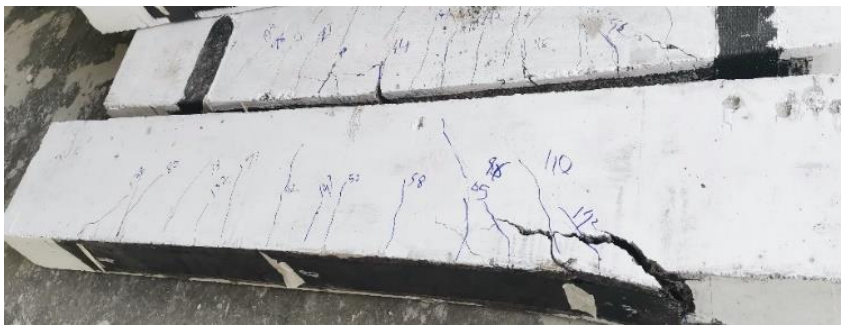

(a)

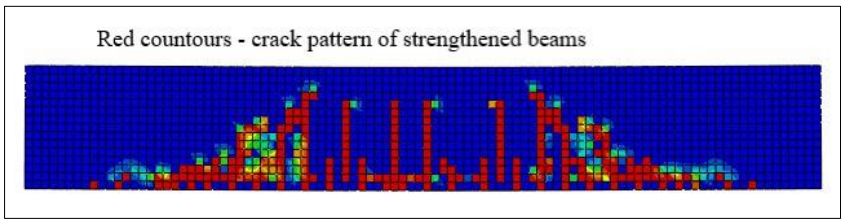

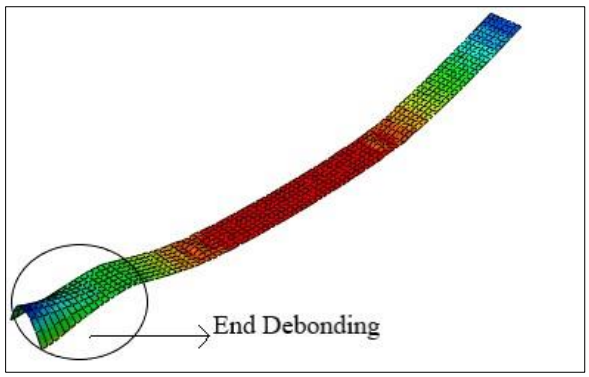

(b)

Figure 13. (a) Failure mode in Specimen CE - Concrete cover Separation failure, (b) Failure mode in Specimen FE-CE – Plate End debonding

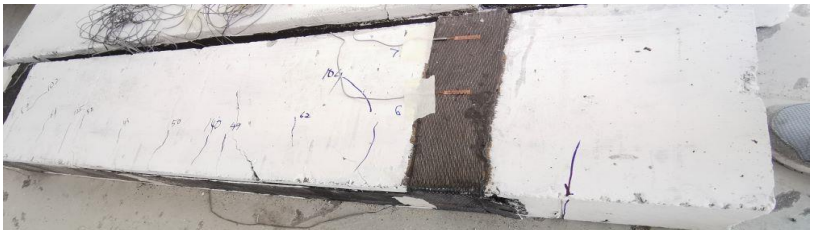

(a)

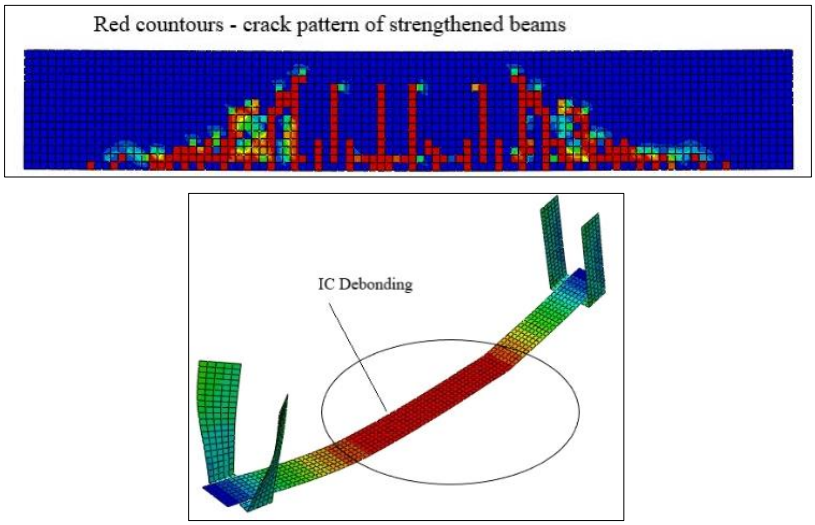

(b)

Figure 14. (a) Failure mode in specimen CU – IC debonding, (b) Failure mode in specimen FE-CU – IC debonding of longitudinal CFRP and debonding of U-wraps

The specimens ABU1 and ABU2, strengthened with longitudinal CFRP and alternative U-wrap end anchorages, outperformed the CU specimens in load-carrying capacity. Here, the stress concentrations eventually led to FRP anchor rupture and complete debonding of the CFRP soffit plate, as shown in Figure 15-a. Although end debonding did take place during the entire process, the intervention of the end anchorages retarded the propagation of longitudinal CFRP debonding. Test results from the experimental study are summarized in Table 2.

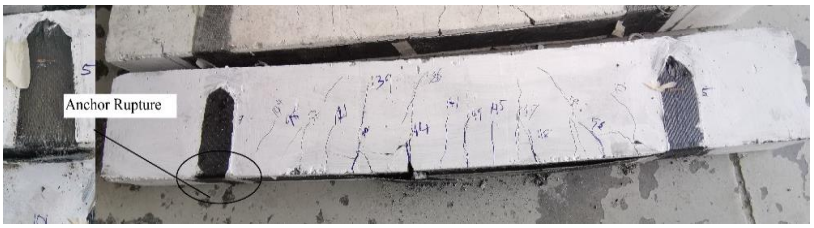

(a)

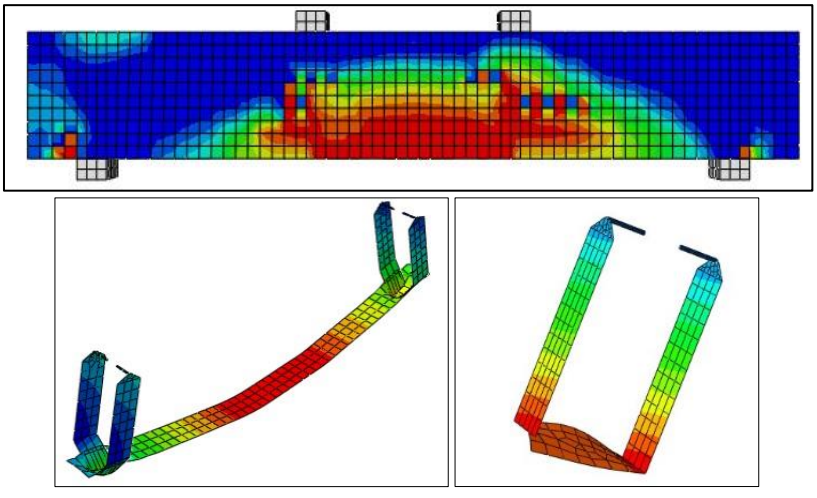

(b)

Figure 15. (a) Failure mode in specimen ABU – CFRP Anchor Rupture followed by debonding of soffit plate, (b) Failure mode in specimen FE-ABU – depicting failure of concrete, longitudinal CFRP and rupture of alternative U-wrap anchors

Table 2. Key Results from Experimental Study

Parameters	CS	CE		CU		AB-U	
	CS-1	CE-1	CE-2	CU-1	CU-2	AB-U1	AB-U2
Peak Load, kN	135.1	155.9	149	173.51	175	194.45	198.1
Yield Load displacement, mm	5.35	3.85	3.9	5.7	5.4	4.7	5
Peak load displacement, mm	21.25	6.73	6.9	11.7	11.9	13.1	12.6
Load increase (%)	--	15.4	10.3	28.4	29.5	44	46.6
Ductility	4	1.75	1.77	2.05	2.2	2.8	2.52
Failure Mode	Flexure	Concrete cover separation (CCS)		Intermediate crack (IC) Debonding		CFRP anchor rupture	

3.3. Load-CFRP Strain

All the CFRP-strengthened samples were equipped with strain gauges, which were attached to the data acquisition system. The midspan strain readings of longitudinal CFRP were recorded and plotted against the load to identify failure modes and strain compatibility. The load versus CFRP strain relations of CE, CU, and AB-U specimens are shown in Figure 16. All the specimens exhibited trilinear behavior. In the first phase, the diagram shows a linear behavior, but there is no significant increase in CFRP strain with increasing load, indicating a lower contribution of the CFRP in this phase. The second phase showed a significant increase in CFRP strain with increasing load up to a certain threshold value, which varied among the specimens. The increase in the recorded strain values for CU and AB-U specimens compared to CE specimens indicates the efficiency of the end anchors. The sudden drop in the curve for CE specimens signifies cover separation failure. The peak strain recorded for CE specimens was 2735 με. A significant increase in the maximum FRP failure strain to 4980 με was observed for CU specimens (82.1 % higher than for CE specimens). The AB-U specimens exhibited a maximum strain of 7615 με. Compared to CU specimens, a 53% higher CFRP strain was observed in the AB-U specimens, indicating that the applied U-wrap scheme significantly increases strain compatibility and load-bearing capacity.

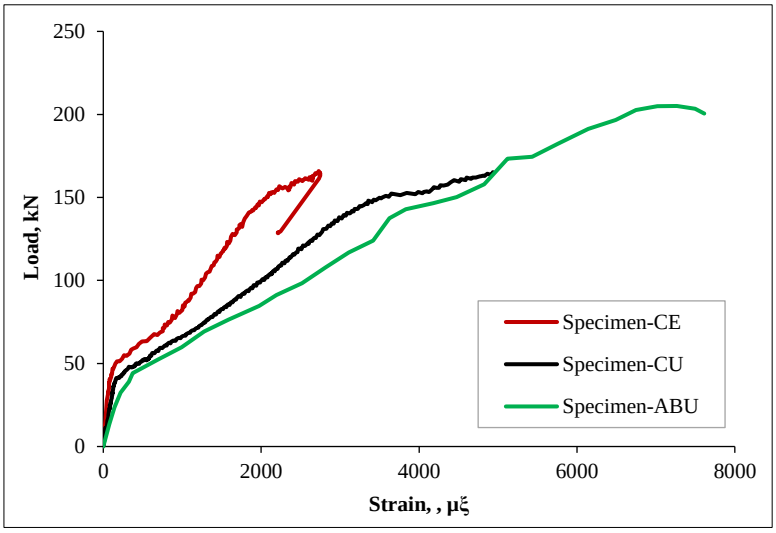

Figure 16. Load v/s FRP midspan strain relationship of tested specimens

3.4. Ductility

Ductility in structures is a critical property and can be defined as the ability of a structure to undergo significantly larger deformations while maintaining its load-carrying capacity. Displacement ductility is quantified as the ratio of ultimate deflection to deflection at steel yielding [22]. The ductility of components is reduced when using CFRP reinforcement compared to unstrengthened samples. The brittle debonding failure in FRP-strengthened specimens causes this significant reduction in their ductility. The alternative U-wrap anchor is designed to improve the ductility performance of CFRP-strengthened specimens. The ductility of the specimens is shown in Table 2. The CE specimens exhibit the lowest ductility. Comparing the values of the CE beams with those of the CS beams (reference beams), there is a significant decrease from 4 to 1.76, indicating that the ductility is 56% lower than that of the control specimens. An improvement in ductility was observed when end anchors were used. The average ductility of the specimens with conventional U-jacket end anchoring (CU specimens) was 2.1, representing a 19.3% improvement compared to the ductility of the unanchored specimens (CE specimens). A significant increase in ductility was observed when alternative U-wraps were used as end anchorage. The average ductility of the specimens was 2.7, which is 28.6% higher than that of the CU specimens. This can be possibly due to the rupture of the anchors and improvement in deformation of AB-U specimens.

4. Finite Element Study

Numerical simulation studies are conducted to assess the accuracy of the strengthening scheme. Nonlinear finite element (FE) analyses are performed using the versatile finite element software ABAQUS. For this purpose, four full-scale numerical models are created and analyzed with loading and boundary conditions identical to those of the experimental study. The load-deflection behavior and failure modes of the models are then compared with the experimental results.

4.1. Material Property and Element Types

To model the concrete beam, a linear eight-noded brick element with 3 active degrees of freedom per node - C3D8R is used. The inelastic behavior and damage of concrete both in compression and tension is simulated using a Concrete Damage Plasticity (CDP) model available in ABAQUS library. The model considers the isotropic elastic damage and material's plastic behavior, which enable it to simulate the tensile cracking and compressive concrete crushing [23]. The elastic modulus (E_c) and tensile strength (f_t) for the concrete beam are calculated from the experimental studies. The material properties of concrete are given in Table 3, and the damage parameters of the CDP model are given in Table 4.

Table 3. Material properties - Concrete

Compressive Strength	Elastic Modulus	Poisson's ratio	Tensile strength
50 MPa	36.3 GPa	0.2	4.33 MPa

Table 4. Damage Parameters of CDP model

Damage Parameters	Dilation angle	Eccentricity	f_{b0}/f_{c0}	K	Viscosity parameter
Value	36	0.1	1.16	0.67	0.02

where, K and f_{b0}/f_{c0} are the ratio of second stress invariant on tensile meridian and ratio of biaxial to uniaxial compressive strength and, respectively.

The internal steel rebars are assumed to have an elastic-plastic behavior with linear strain-hardening characteristics. A two-noded linear displacement truss element T3D2 (with 3 degrees of freedom) is used to model the compression rebars, tension rebars, and stirrups. Table 5 depicts the properties of steel. The loading and support elements are modeled as a linear elastic tensile model.

Table 5. Material properties - Steel

Steel Diameter (mm)	Elastic modulus (GPa)	Poisson's ratio	Yield Strength (MPa)
10	210 GPa	0.3	528
12	210 GPa	0.3	560

In the study, the CFRP fabric, including longitudinal CFRP, CFRP U-jackets, and alternative U-jackets, is modeled as lamina with linear elastic behavior. A 4-node shell element, S4R, is used, and the shell thickness provided is 0.167 mm. To predict typical failures in FRP sheets like interlaminar shear, fiber or matrix failure, Hashin's damage criteria for composite structures are applied, with Hashin's damage properties referenced from Raza et al. [24]. The elastic properties of the CFRP fabrics are detailed as follows: the elastic modulus is 220 GPa in the longitudinal direction and 16.6 GPa in the transverse direction, while the Poisson's ratio is 0.3.

4.2. Modeling of CFRP-Concrete Interface

A perfect bond is assumed between the concrete substrate and the internal steel rebars, as no detachment of the steel was observed during the experimental study. Hence, embedded constraints are applied between concrete and reinforcement. The interaction between the load plates and the concrete substrate is simulated using a tie-constraint. However, assuming a perfect bond between the concrete substrate and the CFRP elements may result in potentially overestimated results as they are not able to capture debonding failures. To address this, cohesive zone modeling is used to simulate the CFRP-concrete interface. For this purpose, an eight-noded three-dimensional cohesive element, COH3D8, is employed to provide more accurate results. The cohesive surface is modeled using a bilinear traction-separation law. Figure 17 depicts the graphical representation of this bilinear traction-separation law, which consists of three distinct phases: the initial linear elastic behavior, the point of damage initiation, and the damage evolution zone defined in terms of fracture energy (the linearly softening portion).

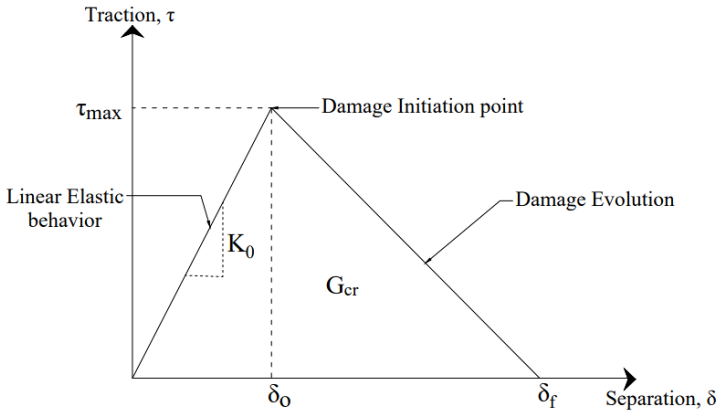

Figure 17. Bilinear traction-separation law

The relationship between traction and separation can be defined in terms of the initial stiffness, K_0 (given by the Equation 1), shear strength of interface τ_{max} (given by Equation 2), fracture energy G_{cr} (area under the curve) [25].

$$K_0 = \frac{1}{\left(\frac{t_i}{G_i}+\frac{t_c}{G_c}\right)} \quad (1)$$

$$\tau_{max} = 1.5\beta_w f_t \quad (2)$$

where t_c and t_i are the thickness of concrete and resin respectively and G_i is the shear modulus of resin and G_c is the shear modulus of concrete. β_w is given by Equation 3 and f_t is tensile strength of concrete.

$$\beta_w = \sqrt{\frac{2.25-\left(b_f/b_c\right)}{1.25+\left(b_f/b_c\right)}} \quad (3)$$

where, b_f and b_c are thickness of CFRP and concrete respectively.

Fracture energy can be defined as a cohesive interaction feature and can be specified in tabular form, using linear or exponential softening behavior, or by employing the Benzeggagh-Kenane (BK) form [26]. Abaqus ensures that the fracture energy corresponds to the area under the linear or exponential damage response. In this investigation, the Benzeggagh-Kenane (BK Law) form is utilized.

4.3. Boundary Conditions and Loading

To create simply supported boundary conditions, constraints were applied to the support elements. On one element set, constraints are applied to restrict translation in all three directions (X, Y, and Z). On the other hand, translation is only restricted in the Y direction on the second support element set. A two-point loading setup was created on the loading plates, and displacement-controlled loading at 1.5 mm/sec is provided. For all the numerical models, a finite mesh of size 5 mm was applied to get accurate results. The meshed models are shown in Figures 18 and 19. After this, numerical simulation is carried out, and results are viewed in the post processing module.

5. Numerical Results and Validation

The key focus of the numerical investigations is to evaluate the effectiveness of the finite element analysis in modelling the behavior of beams strengthened with CFRP in flexure. Simulation studies were conducted on four models with different strengthening configurations to assess the accuracy of the proposed alternative U-wrap anchoring technique. These models include: an unstrengthened control specimen (FE-CS), a specimen with longitudinal CFRP on the tension side (FE-CE), a specimen with both longitudinal CFRP and a CFRP U-jacket (FE-CU), and a specimen with longitudinal CFRP secured with the alternative U-jacket (FE-ABU).

5.1. Model Validation and Discussion of Results

The L-D curves obtained from the simulation analysis at the mid-span of the numerical models are shown in Figure 20-a to 20-d. To verify the accuracy of the finite element (FE) analysis, the results of the numerical study are compared with the experimental results. The figures demonstrate that the numerical response of the models, in terms of load-carrying capacity, agrees well with the experimental results. This confirms the model's ability to predict the behaviour of strengthened beams. The results indicate that CFRP reinforcement and the use of end anchors enhance the

performance of the specimens by increasing their load-bearing capacity. The numerical models also show slightly increased stiffness, which can be attributed to the assumption of perfect interaction between the concrete and the reinforcement assembly. The ratio of the experimental to the numerical results for load-bearing capacity is within 5%. The figures clearly show that the numerical model accurately predicts the beams' behaviour at cracking, yielding of tension rebars, and delamination failures. Table 6 presents the obtained results, including the nomenclature of the numerical models.

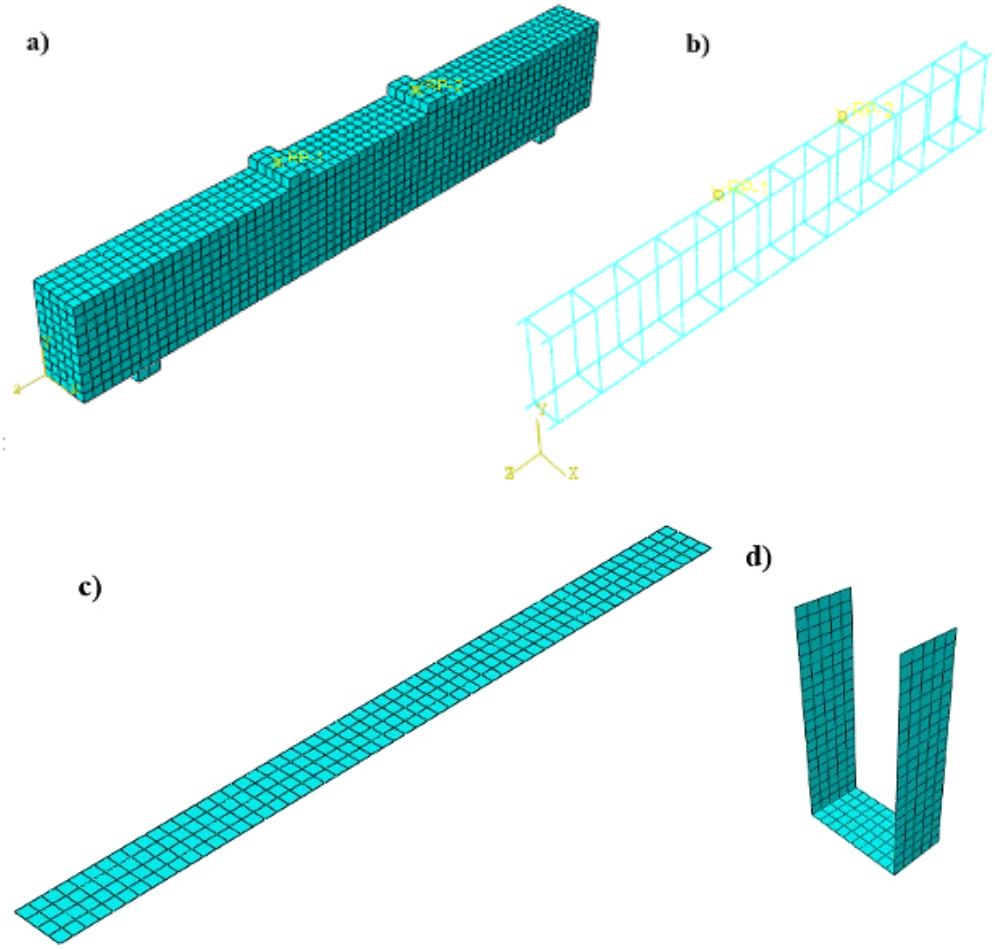

Figure 18. Meshed Models of CE and CU specimens: a) RC beam model with load plates and support elements b) Reinforcement Assembly c) CFRP soffit plate d) CFRP U-jackets

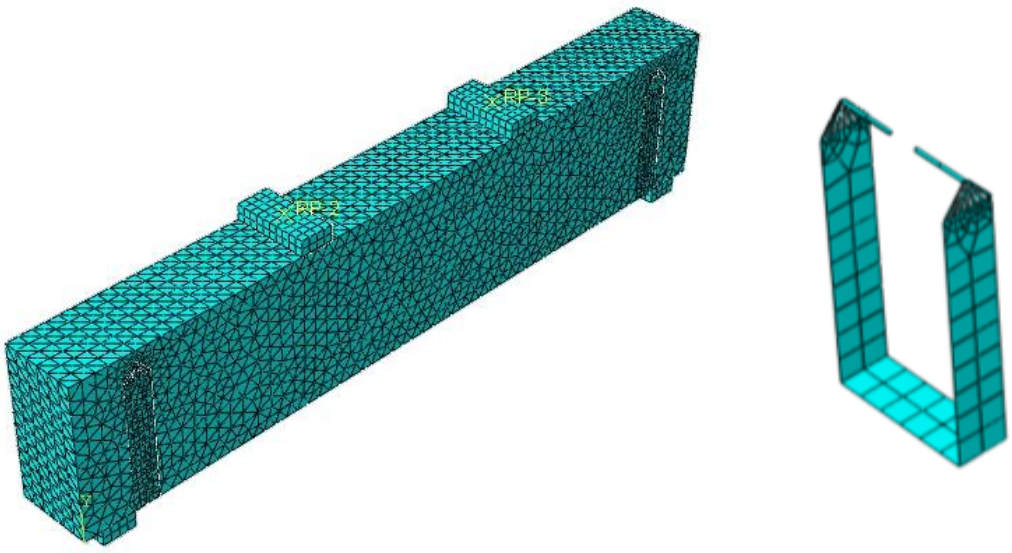

(a) (b)

Figure 19. Meshed Models (a) F-AB-U Specimens, (b) Alternate U-wrap

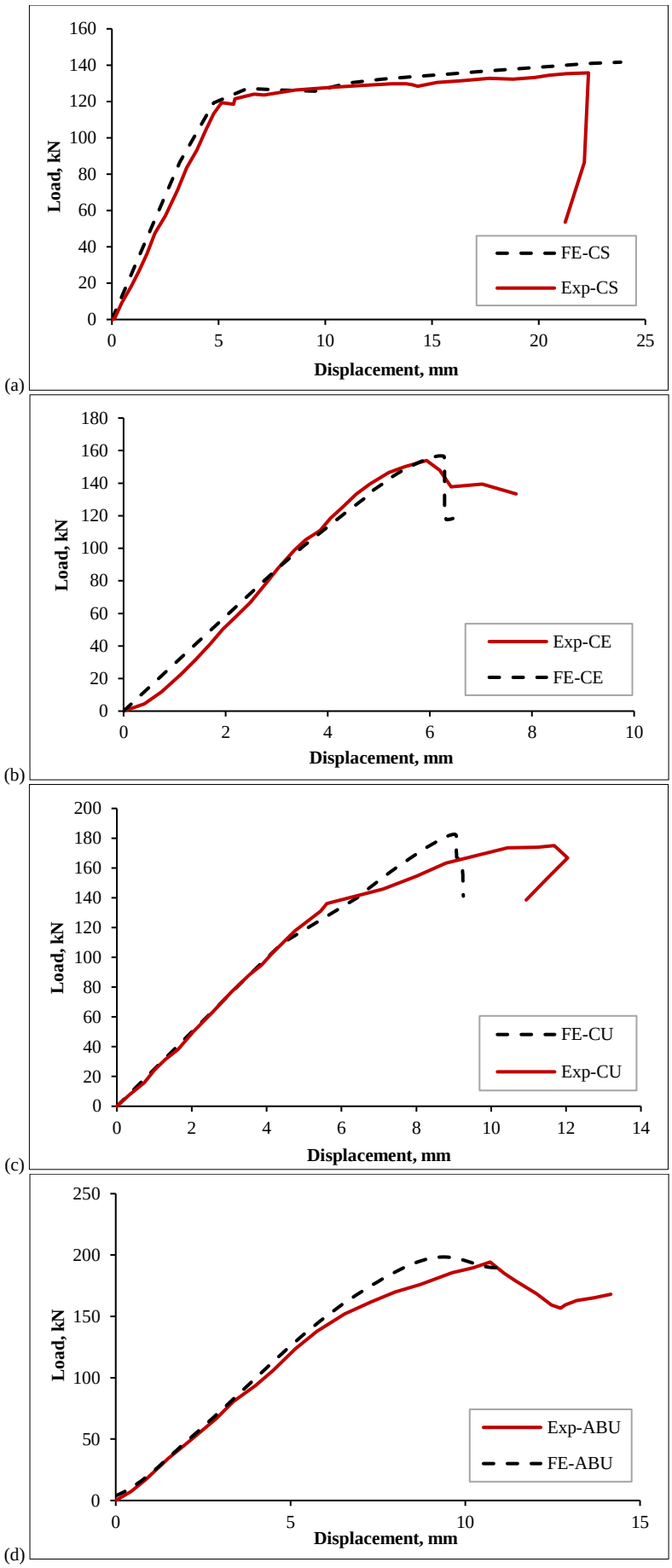

Figure 20. (a) Comparison of Load deflection behavior- Control Specimen, (b) Comparison of Load deflection behavior- Specimen CE and FE-CE, (c) Comparison of Load deflection behavior- Specimen CU and FE-CU, (d) Comparison of Load deflection behavior- Specimen AB-U and FE-ABU.

Table 6. Numerical Results

Specimen ID-Experimental	Specimen ID-FE Study	Ultimate Load (kN) - Experimental (avg)	Ultimate Load (kN) - FE study	P_{num}/P_{exp}
CS - Control	FE-CS	135.1	140.8	1.04
CE	FE-CE	152.5	155.9	1.02
CU	FE-CU	174.3	181.68	1.04
AB-U	FE-AB	196.3	201.7	1.03

To provide more precise and accurate solutions, the CFRP-concrete interface is modeled using cohesive elements. In this study, the cohesive element has a finite thickness, and the top and bottom of the element are attached to concrete and CFRP, respectively, using a tie-constraint. All the numerical models exhibited failure modes similar to those of experimental specimens. Figures 12 to 15 show the comparison of failure modes observed in both experimental and Abaqus studies. The FE-CS1 showed flexural failures with a crack pattern similar to that of the CS-1 specimen of the experimental study (as shown in Figure 12 -b). Plate end debonding is noticed in FE-CE specimens, while the FE-CU specimens depict IC debonding (Figure 13-b). The failure mode noted in CE specimens was CCS failure. To achieve this, modeling cohesive elements below the tensile steel and concrete cover may be utilized, as suggested by Al-Saawani et al. [13]. In the FE-CU model, U-wraps also experienced IC debonding as cohesive modeling between U-wraps and beam sides was incorporated (Figure 14-b). For specimens equipped with alternative U-wrap anchors (FE-ABU), anchor rupture was identified, followed by debonding of the longitudinal CFRP, which aligns well with the experimental results (as shown in Figure 15-b).

5.2. Results from Previous Literature Review

Studies have confirmed that the majority of failures occurring in EB-FRP retrofitted beams are due to sudden debonding failures. To improve the strengthening characteristics and ductility of these beams, end anchorages have been introduced. Mostofinejad et al. [20] proposed a novel method called the "warp and woof method" to enhance the efficiency of conventional U-wrap end anchorages. This method ensures direct contact between the anchors and the tension side of the concrete beam. It demonstrated improved load capacity, a shift of debonding failures to longitudinal CFRP rupture, and an increase in ductility. Esmaeili et al. [27] conducted experimental and analytical studies on a novel plate anchorage system consisting of two steel plates directly welded to the tensile reinforcement using steel angles. All specimens with the proposed anchorage system failed due to FRP sheet rupture, and an increase in load capacity was observed. Mostafa & Razaqpur [28] designed a one-piece anchor known as FRP π- anchor which consists of a monolithically built FRP head plate partially bonded to a substrate and two steel shanks that are inserted into epoxy filled precut holes. These anchors effectively resist FRP pullout/delamination and high shear stresses at the interface, increasing the load-carrying capacity. Yahiaoui et al. [29] evaluated the effectiveness of a bolt end anchoring system. To enhance the bond behavior between GFRP sheets and the concrete substrate, GFRP anchoring plates are connected to the bottom using bolts. This significantly improved the elasticity, stiffness, and energy absorption of the retrofitted beams. Al-Saawani et. al. [16] studied the effect of using inclined U-wrap anchors by varying the width of the anchor. They concluded that anchors with increased width or area can improve load capacity and prevent concrete cover separation failure.

All the studies discussed in this section were aimed at overcoming the disadvantages of conventionally available anchors to eliminate catastrophic debonding. The load capacity of the anchored specimens in the current investigation is compared with that of the control specimens and with the results from the literature depicted in Figure 21. The results of the ultimate load of anchored specimens (P_anchored) are compared to the ultimate load of control specimens (P_control). To improve and optimize the suggested anchoring technique, parametric studies are to be conducted.

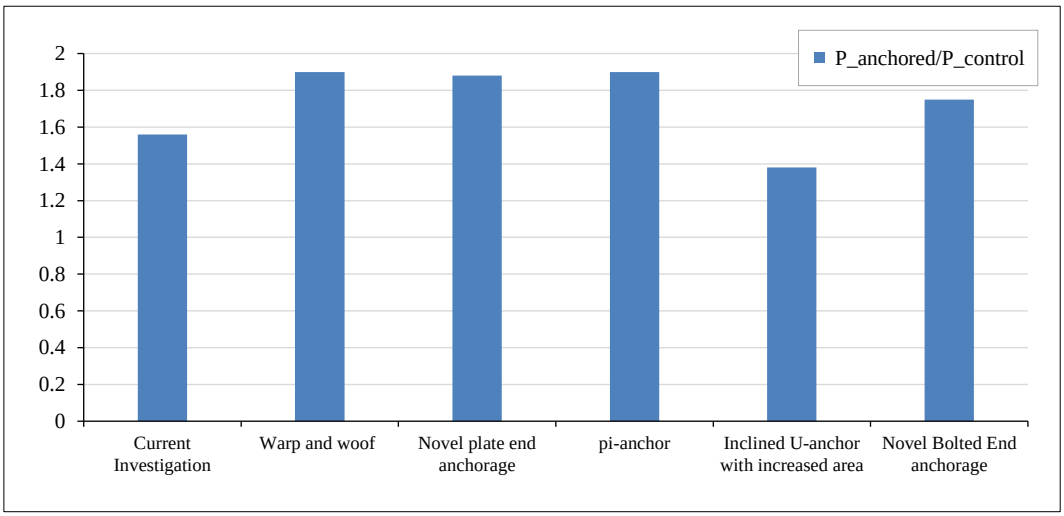

Figure 21. Comparison of test results with previous literature

6. Conclusions

This This study investigates the behavior of RC beams externally strengthened with CFRP soffit plates and end anchorages under flexure. An alternative CFRP U-wrap anchorage is introduced in the study, and the performance of the anchorage is evaluated. For this purpose, seven beams of size 1.96 × 0.15.0.3 m were tested under four-point bending. The performance of specimens in terms of load displacement, modes of failure, FRP strains, and ductility is studied and compared with the existing U-jacket anchorage technique. Full-scale numerical models were created using FE software Abaqus and are validated by the experimental results. The conclusions of the study are summarized below:

- The implementation of alternative U-jackets as end anchorages has significantly enhanced structural performance by improving the confinement and increasing the flexural capacity of the specimens.
- The capability of CFRP longitudinal strips could be maximized by using the suggested alternative U-wrap anchoring techniques. By implementing this anchorage technique, the AB-U beam specimens demonstrated increased average load-bearing capacity, which is 45.3% more than that of the control specimen CS1 and 13% more than that of CU specimens.
- The premature debonding failures that were identified in the CE and CU specimens, characterized by concrete cover separation and IC debonding, were successfully shifted to the failure of CFRP anchor in the AB-U specimens. By incorporating alternative U-wrap anchorages, the longitudinal CFRP gets an additional confinement, which enhances the CFRP-concrete bond, enabling effective load transfer.
- The alternative U-anchoring method utilized in AB-U specimens showed enhanced ductility and strain compatibility when compared to CE and CU specimens.
- Simulation studies carried out utilizing the Concrete Damage Plasticity approach and cohesive zone modeling are found to be in good agreement with the experimental study in terms of load-deflection behavior.

In conclusion, the combination of CFRP soffit plates and alternative U-jackets presents a viable method for improving the load carrying capability and strain compatibility of RC beams. The developed FE models can be used to further explore the behavior by conducting various parametric studies.

7. Declarations

7.1. Author Contributions

Conceptualization, S.M.V.; methodology, S.M.V. and S.R.S.; software, S.M.V.; validation, S.M.V.; formal analysis, K.K.; resources, S.M.V. and S.R.S.; writing—original draft preparation, S.M.V.; writing—review and editing, K.K.; visualization, R.S.; supervision, K.K. and R.S.S.; project administration, S.R.S.; funding acquisition, Y.Y. All authors have read and agreed to the published version of the manuscript.

7.2. Data Availability Statement

The data presented in this study are available in the article.

7.3. Funding

The authors received no financial support for the research, authorship, and/or publication of this article.

7.4. Conflicts of Interest

The authors declare no conflict of interest.

8. References

[1] El-Mandouh, M. A., Hu, J. W., Shim, W. S., Abdelazeem, F., & ELsamak, G. (2022). Torsional Improvement of RC Beams Using Various Strengthening Systems. Buildings, 12(11), 1776. doi:10.3390/buildings12111776.

[2] Askar, M. K., Hassan, A. F., & Al-Kamaki, Y. S. S. (2022). Flexural and shear strengthening of reinforced concrete beams using FRP composites: A state of the art. Case Studies in Construction Materials, 17. doi:10.1016/j.cscm.2022.e01189.

[3] Ceroni, F. (2010). Experimental performances of RC beams strengthened with FRP materials. Construction and Building Materials, 24(9), 1547–1559. doi:10.1016/j.conbuildmat.2010.03.008.

[4] ACI 440.2R-17 (2017). Guide for the Design and Construction of Externally Bonded FRP Systems for Strengthening Concrete Structures. American Concrete Institute (ACI), Michigan, United States. doi:10.14359/51700867.

[5] Chalioris, C. E., Zapris, A. G., & Karayannis, C. G. (2020). U-jacketing applications of fiber-reinforced polymers in reinforced concrete t-beams against shear-tests and design. Fibers, 8(2), 13. doi:10.3390/fib8020013.

[6] Elsayed, W. E., Ebead, U. A., & Neale, K. W. (2009). Studies on mechanically fastened fiber-reinforced polymer strengthening systems. ACI Structural Journal, 106(1), 49–59. doi:10.14359/56283.

[7] Al-Atta, B., Kalfat, R., & Al-Mahaidi, R. (2022). Hybrid and patch anchors for prevention of IC debonding in RC planks flexurally strengthened using FRP. Structures, 43, 1042–1056. doi:10.1016/j.istruc.2022.07.026.

[8] Sun, W., Liu, S., & Zhang, C. (2020). An effective improvement for enhancing the strength and feasibility of FRP spike anchors. Composite Structures, 247. doi:10.1016/j.compstruct.2020.112449.

[9] Abdalla, J. A., Mhanna, H. H., Ali, A. B., & Hawileh, R. A. (2023). CFRP U-Wraps and Spike Anchors for Enhancing the Flexural Performance of CFRP-Plated RC Beams. Polymers, 15(7), 1621. doi:10.3390/polym15071621.

[10] Chen, W., Pham, T. M., Sichembe, H., Chen, L., & Hao, H. (2018). Experimental study of flexural behaviour of RC beams strengthened by longitudinal and U-shaped basalt FRP sheet. Composites Part B: Engineering, 134, 114–126. doi:10.1016/j.compositesb.2017.09.053.

[11] Al-Saawani, M. A., El-Sayed, A. K., & Al-Negheimish, A. I. (2022). Mitigation of Concrete Cover Separation in Concrete Beams Strengthened with Fiber-reinforced Polymer Composites. IOP Conference Series: Earth and Environmental Science, 1026(1), 12008. doi:10.1088/1755-1315/1026/1/012008.

[12] Fu, B., Teng, J. G., Chen, J. F., Chen, G. M., & Guo, Y. C. (2017). Concrete Cover Separation in FRP-Plated RC Beams: Mitigation Using FRP U-Jackets. Journal of Composites for Construction, 21(2), 04016077. doi:10.1061/(asce)cc.1943-5614.0000721.

[13] Al-Saawani, M. A., El-Sayed, A. K., Al-Negheimish, A. I., & Alhozaimy, A. M. (2024). FRP U-Wraps for Mitigating Plate-End Debonding in FRP-Strengthened Beams: Finite Element Modeling and Parametric Study. Arabian Journal for Science and Engineering, 49, 14001–14019. doi:10.1007/s13369-024-08853-6.

[14] Fu, B., Tang, X. T., Li, L. J., Liu, F., & Lin, G. (2018). Inclined FRP U-jackets for enhancing structural performance of FRP-plated RC beams suffering from IC debonding. Composite Structures, 200, 36–46. doi:10.1016/j.compstruct.2018.05.074.

[15] Al-Mahaidi, R., & Kalfat, R. (2018). FRP Anchorage Systems. Rehabilitation of Concrete Structures with Fiber-Reinforced Polymer, 331–376. doi:10.1016/b978-0-12-811510-7.00008-2.

[16] Al-Saawani, M. A., El-Sayed, A. K., & Al-Negheimish, A. I. (2023). Inclined FRP U-Wrap Anchorage for Preventing Concrete Cover Separation in FRP Strengthened RC Beams. Arabian Journal for Science and Engineering, 48(4), 4879–4892. doi:10.1007/s13369-022-07186-6.

[17] Dong, J., Wang, Q., & Guan, Z. (2013). Structural behaviour of RC beams with external flexural and flexural-shear strengthening by FRP sheets. Composites Part B: Engineering, 44(1), 604–612. doi:10.1016/j.compositesb.2012.02.018.

[18] Ceroni, F., & Pecce, M. (2005). Ductility performance of RC beams strengthened with CFRP sheets. WIT Transactions on the Built Environment, 81, 579–589.

[19] Ali, A., Abdalla, J., Hawileh, R., & Galal, K. (2014). CFRP mechanical anchorage for externally strengthened RC beams under flexure. Physics Procedia, 55, 10–16. doi:10.1016/j.phpro.2014.07.002.

[20] Mostofinejad, D., Hosseini, S. M., Nader Tehrani, B., Eftekhar, M. R., & Dyari, M. (2019). Innovative warp and woof strap (WWS) method to anchor the FRP sheets in strengthened concrete beams. Construction and Building Materials, 218, 351–364. doi:10.1016/j.conbuildmat.2019.05.117.

[21] Eslami, A., Shayegh, H. R., Moghavem, A., & Ronagh, H. R. (2019). Experimental and analytical investigations of a novel end anchorage for CFRP flexural retrofits. Composites Part B: Engineering, 176. doi:10.1016/j.compositesb.2019.107309.

[22] Bank, L. C. (2013). Progressive Failure and Ductility of FRP Composites for Construction: Review. Journal of Composites for Construction, 17(3), 406–419. doi:10.1061/(asce)cc.1943-5614.0000355.

[23] Xiao, Y., Chen, Z., Zhou, J., Leng, Y., & Xia, R. (2017). Concrete plastic-damage factor for finite element analysis: Concept, simulation, and experiment. Advances in Mechanical Engineering, 9(9), 1–10. doi:10.1177/1687814017719642.

[24] Raza, A., Khan, Q. uz Z., & Ahmad, A. (2020). Prediction of Axial Compressive Strength for FRP-Confined Concrete Compression Members. KSCE Journal of Civil Engineering, 24(7), 2099–2109. doi:10.1007/s12205-020-1682-x.

[25] Obaidat, Y. T., Heyden, S., & Dahlblom, O. (2010). The effect of CFRP and CFRP/concrete interface models when modelling retrofitted RC beams with FEM. Composite Structures, 92(6), 1391–1398. doi:10.1016/j.compstruct.2009.11.008.

[26] Benzeggagh, M. L., & Kenane, M. (1996). Measurement of mixed-mode delamination fracture toughness of unidirectional glass/epoxy composites with mixed-mode bending apparatus. Composites Science and Technology, 56(4), 439–449. doi:10.1016/0266-3538(96)00005-x.

[27] Esmaeili, J., Aghdam, O. R., Andalibi, K., Kasaei, J., & Gencel, O. (2022). Experimental and numerical investigations on a novel plate anchorage system to solve FRP debonding problem in the strengthened RC beams. Journal of Building Engineering, 45. doi:10.1016/j.jobe.2021.103413.

[28] Mostafa, A. A. B., & Razaqpur, A. G. (2013). A new CFRP anchor for preventing separation of externally bonded laminates from concrete. Journal of Reinforced Plastics and Composites, 32(24), 1895–1906. doi:10.1177/0731684413498633.

[29] Yahiaoui, D., Boutrid, A., Saadi, M., Mamen, B., & Bouzid, T. (2023). New Anchorage Technique for GFRP Flexural Strengthening of Concrete Beams Using Bolts-End Anchoring System. International Journal of Concrete Structures and Materials, 17(1), 20. doi:10.1186/s40069-023-00578-4.